ELSEVIER

Soil Dynamics and Earthquake Engineering 19 (2000) 333–338

SOIL DYNAMICS AND EARTHQUAKE ENGINEERING

www.elsevier.com/locate/soildyn

Simulation of liquefaction beneath an impermeable surface layer

N. Yoshida[a], W.D.L. Finn[b,*]

[a]*Sato Kogyo Company Ltd, Tokyo, Japan*

[b]*Anabuki Chair of Foundation Geodynamics, Kagawa University, Hayashi-cho, 2217-20 Shinmachi, Takamatsu 761-0396, Japan*

Accepted 6 May 2000

Abstract

A joint element is proposed, which can simulate the three phases of behaviour of an impermeable layer over a liquefied sand layer. The analysis tracks the post-liquefaction reconsolidation of the sand, the simultaneous development of a water film between the layers and the settlements resulting from the subsequent drainage of the water film. The element is incorporated in a finite element program, which can be used to simulate the behaviour of layered systems. The effectiveness of the program is demonstrated by simulation of the performance of a model soil deposit of two layers in a centrifuge test. © 2000 Elsevier Science Ltd. All rights reserved.

Keywords: Liquefaction; Reconsolidation; Joint element; Interface behaviour

1. Introduction

Lateral spreading of the ground and flow failures of embankments are two of the major hazards associated with liquefaction of saturated sands. In these cases, the resistance to movement relies substantially on the residual or steady state strength of the liquefied sand. However, in one instance, this strength may not be available soon after liquefaction. When the liquefied sand is covered by an impermeable layer, water will accumulate below it as the sand reconsolidates after liquefaction. Until the impermeable layer cracks and allows drainage of the accumulated water, there is no shearing resistance under the impermeable layer.

If the impermeable layer is sloping, a flow failure may occur. This type of failure is of serious concern in the case of earth dams, where often a relatively impermeable embankment surrounds a zone of liquefiable sand. This hazard has led to model studies using centrifuge tests to provide data for understanding and modelling such phenomena [1]. The detailed 2D analysis of this phenomenon from initial seismic excitation to the final post-liquefaction state is beyond our present capacity.

In this paper, a beginning is made towards modelling the behaviour of a relatively impermeable surface layer over a liquefied sand layer. A method of analysis is developed for the 1D case of a horizontal layered deposit. Liu and Dobry [2] tested such a soil deposit in a centrifuge test in which accelerations, porewater pressures and settlements were monitored continuously. Data from this test provides a clear picture of what happens at the interface between the layers following liquefaction and the means of the data for validating proposed models for simulating the response of the system.

The basis of the proposed method is a joint element that simulates interface behaviour and that can be incorporated in a finite element code for seismic response analysis. The objectives of this paper are to describe the theory of such an element and demonstrate its capability to model interface behaviour after liquefaction. In what follows, first the joint element is described and the post-liquefaction properties needed for analysis are developed. Then, the behaviour of a model two-layer deposit in a seismic centrifuge test conducted by Liu and Dobry [2] is simulated. The simulation study shows that the joint element is capable of modelling adequately the main features of the effective stress seismic response of a horizontal impermeable layer over a liquefied sand layer.

2. Theory of joint element

2.1. Equilibrium equation

The equations defining the behaviour of the joint element as it accumulates free water in the interface between layers are developed for the case of vertical displacements. This limits the applicability to horizontally layered deposits. The joint element is shown in the open position in Fig. 1.

* Corresponding author.
E-mail address: finn@eng.kagawa-u.ac.jp (W.D.L. Finn).

PII: S0267-7261(00)00018-X

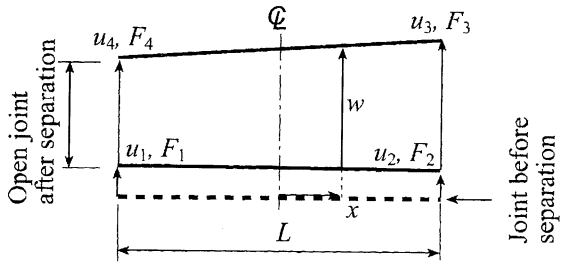

Fig. 1. Geometry of joint element.

Relative displacement between the top and bottom faces of the joint, $w = u_t - u_b$, is given by Eq. (1)

$$w = \{B\}\{u\} \tag{1}$$

Here u_t and u_b are the displacements at the top and bottom faces of the joint element. $\{B\}$, the interpolation function, and $\{u\}$, the nodal displacement vector, are given by

$$\{B\} = \left\{ -\frac{1}{2} + \frac{x}{L} \quad -\frac{1}{2} - \frac{x}{L} \quad \frac{1}{2} + \frac{x}{L} \quad \frac{1}{2} - \frac{x}{L} \right\} \tag{2}$$

$$\{u\} = \{ u_1 \quad u_2 \quad u_3 \quad u_4 \}^{\mathrm{T}} \tag{3}$$

Here x is the co-ordinate along the joint, L is the length of the joint and u_1 to u_4 are the nodal displacements shown in Fig. 1 [3].

The constitutive equation for the joint for relative vertical displacements only is

$$\sigma' = -Sw \tag{4}$$

Here σ' is the effective normal *compressive* stress between the faces of the joint, and S is a parameter connecting effective stress and displacements normal to the joint. It has a large positive value when the joint closes and is zero when the joint opens. Equilibrium between the nodal forces on the joint and the element total stresses σ is expressed by

$$\{F\} = \int_{-L/2}^{L/2} -\{B\}^{\sigma}\,\mathrm{d}x \tag{5}$$

When porewater pressures p develop in the joint, the total stress σ in the joint element is,

$$\sigma = \sigma' + p \tag{6}$$

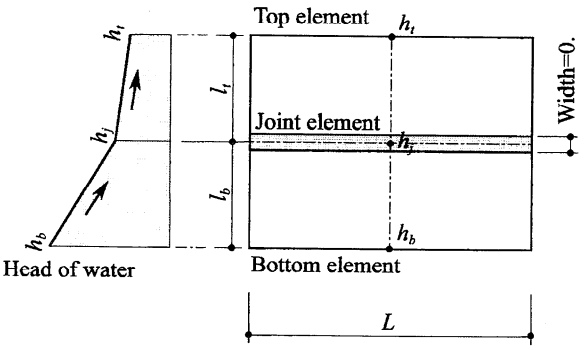

Fig. 2. Porewater pressure conditions around the joint element.

Substitution of Eqs. (1), (4) and (6) into Eq. (5) gives the equilibrium equation of the joint element as

$$\{F\} = [K]\{u\} - \{K_p\}p \tag{7}$$

where $[K]$ is the joint stiffness matrix given by

$$[K] = \frac{SL}{6}\begin{bmatrix} 2 & 1 & -1 & -2 \\ 1 & 2 & -2 & -1 \\ -1 & -2 & 2 & 1 \\ -2 & -1 & 1 & 2 \end{bmatrix} \tag{8}$$

and $\{K_p\}$ is a porewater pressure matrix given by

$$\{K_p\} = \int_{-L/2}^{L/2} \{B\}^{\mathrm{T}}\mathrm{d}x = \frac{L}{2}\{ -1 \quad -1 \quad 1 \quad 1 \}^{\mathrm{T}} \tag{9}$$

2.2. Continuity equation for joint

The volume of water, W, flowing out of the joint element shown in Fig. 2 during the time $\mathrm{d}t$ is given by

$$dW = L\left(k_t \frac{h_t - h_j}{l_t} + k_b \frac{h_b - h_j}{l_b}\right)\mathrm{d}t \tag{10}$$

where h_j denotes the head of water in the joint element, k_t and k_b are the permeabilities of the soil elements contacting the top and bottom faces of the joint, l_t and l_b are the distances to the far faces of these elements as shown in Fig. 2, and h_t and h_b, the associated water heads at these faces. By neglecting the velocity head, h_j is expressed as

$$h_j = \frac{p}{\rho_f g} - \frac{\{X\}^{\mathrm{T}}\{b\}}{g} \tag{11}$$

where p denotes porewater pressure in the joint, ρ_f denotes mass density of porewater, g denotes the acceleration due to gravity, $\{X\}$ denotes the position vector, and $\{b\}$ denotes the gravity force vector.

Volume contraction of the joint element per unit length during the time increment $\mathrm{d}t$ during consolidation is given by $-\dot{w}dt$ or $-\{B\}\{\dot{u}\}\,\mathrm{d}t$, where $\dot{u}$ is the velocity of flow. Integrating along the joint gives the total volume contraction as $-\{K_p\}^{\mathrm{T}}\{\dot{u}\}\,\mathrm{d}t$. The continuity equation is obtained by equating this volume change to the outflow water given by Eq. (10), while taking Eq. (11) into account

$$\{K_p\}^{\mathrm{T}}\{\dot{u}\} = -\dot{W} = \alpha(p - \rho_f\{X\}^{\mathrm{T}}\{b\}) - \sum_i \alpha_i(p_i - \rho_f\{X_i\}^{\mathrm{T}}\{b\}) \tag{12}$$

In this equation

$$\alpha_i = \frac{Lk_i}{\rho_f g l_i}, \qquad \alpha = \sum_i \alpha_i \tag{13}$$

where i indicates the top or bottom element forming the joint. Summation is conducted for both sides of the joint

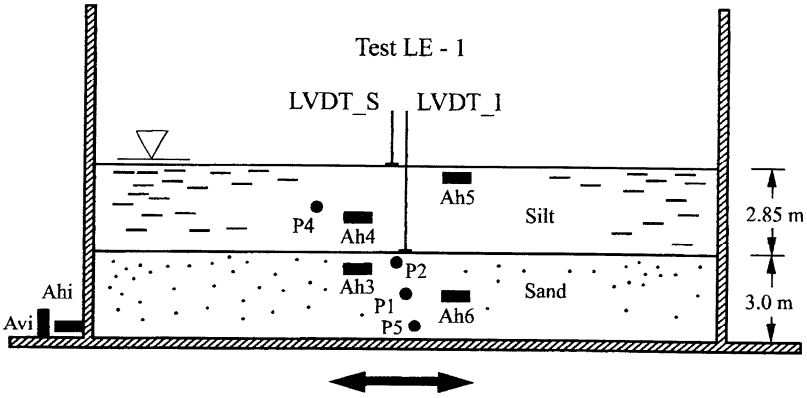

Fig. 3. Centrifuge model test at prototype scale showing the locations of horizontal accelerometers (A_h) and porewater pressure transducers (P) (after Ref. [2]).

element. The incremental forms of Eqs. (7) and (12), used in subsequent analyses, are given by Eqs. (14) and (16), respectively

$$[K]\{du\} - \{K_p\}dp = \{dF\} \tag{14}$$

where

$$dp = p(t + dt) - p(t) \tag{15}$$

and

$$\{K_p\}^T\{du\} - \alpha p\, dt + \sum \alpha_i p_i\, dt = [-\alpha\rho_f\{X\}^T\{b\} + \sum \alpha_i\rho_f\{X_i\}^T\{b\}]dt \tag{16}$$

The Liu and Dobry [2] test, which will be analysed later, has a 1D displacement field. For this case, Eqs. (14) and (16) may be reduced to

$$S\, dw + dp = 0 \tag{17}$$

and

$$dw - \alpha p\, dt + (\alpha_t p_t + \alpha_b p_b)\, dt = -\alpha z\rho_f g dt + \rho_f g(\alpha_t z_t + \alpha_b z_b)dt \tag{18}$$

per unit length of joint. In Eq. (18), z, z_t and z_b are co-ordinates. For the post-liquefaction case, when the joint is open, the change in external load is assumed to be zero. Eliminating the relative displacement $dw = du_t - du_b$ from Eqs. (17) and (18) gives

$$dp = -S\alpha p dt + S(\alpha_t p_t + \alpha_b p_b)\, dt + S\alpha z\rho_f g dt - S\rho_f g(\alpha_t z_t + \alpha_b z_b)dt \tag{19}$$

3. Modelling of volume change characteristics of sand after liquefaction

In order to predict the separation of the joint element or the thickness of the water film, the post-liquefaction volume change characteristics of the sand during dissipation of porewater pressure must be known. Since the occurrence of liquefaction destroys the initial structure of the sand skeleton, the properties before the occurrence of liquefaction are not applicable in post-liquefaction analysis.

Inadomaru et al. [4] conducted cyclic triaxial tests on Toyoura sand in which the volume changes were measured during the dissipation of excess porewater pressure and plotted against the effective mean normal stress. Analysis of these data suggests that the relationship between effective stress and volumetric strain during reconsolidation after liquefaction may be described adequately by

$$\sigma'_m = D(e^{\epsilon_v/c} - 1) \tag{20}$$

where D and c are parameters that define the shapes of the reconsolidation curves, and ϵ_v is the recovered volumetric strain at σ'_m. The (-1) term ensures that the recoverable volumetric strain, ϵ_v, can be initialised at zero for the immediate post-liquefaction condition when $\sigma'_m = 0$. For the test data on Toyoura sand [4], the following expression for c is obtained

$$c = 0.0007 + 0.053\epsilon_{vo} \tag{21}$$

where ϵ_{vo} is the total recovered strain. When c is known, the constant D can be found from

$$D = \frac{\sigma'_{mo}}{e^{\epsilon_{vo}/c} - 1} \tag{22}$$

The 1D compressive modulus for reconsolidation, E_r, is obtained by differentiating Eq. (20) with respect to the volumetric strain, giving

$$\frac{d\sigma'_m}{d\epsilon_v} = \frac{\sigma'_m + D}{c} = E_r \tag{23}$$

4. Numerical example

4.1. Modelled centrifuge test

Liu and Dobry [2] conducted a centrifuge test at $50g$ acceleration on the model of two-layered level ground

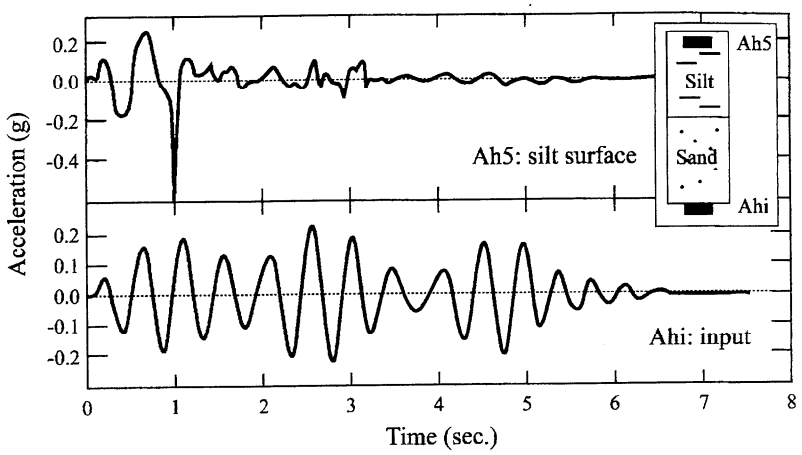

Fig. 4. Acceleration time histories of input and surface motions (after Ref. [2]).

shown in Fig. 3 at prototype scale. A 2.85 m silt layer overlies a 3 m sand layer and the water table is just above the surface of the silt. The locations of accelerometers, porewater pressure gauges, and LVDTs are also shown in Fig. 3. Unit weights of silt and sand are 18.9 and 19.2 kN/m^3, respectively. The relative density of the sand D_r is 40%. Permeability is estimated to be 1×10^{-5} cm/s for silt and 2.13×10^{-3} cm/s for sand on the basis of laboratory permeability tests. The centrifuge was operated at an acceleration of 50g so that the corresponding prototype permeabilities are 5×10^{-6} cm/s and 1.065×10^{-5} cm/s. This test will be used to verify the capability of the analysis described above.

The input accelerations have a peak value of about 0.2g and a duration of about 6 s at prototype scale as shown in Fig. 4. The surface acceleration record shows a significant drop in amplitude after about 1 s of shaking indicating that liquefaction has occurred.

Fig. 5 shows the distribution of excess porewater pressures with depth at different times based on readings from the four porewater pressure transducers. Liquefaction is judged to occur before 5 s, which is consistent with the form of the acceleration record. Note that the porewater pressures remain essentially constant from 15 s to 4.5 min after liquefaction. Time histories of porewater pressure and settlement are presented in Section 4.2, which describes the simulation of the test.

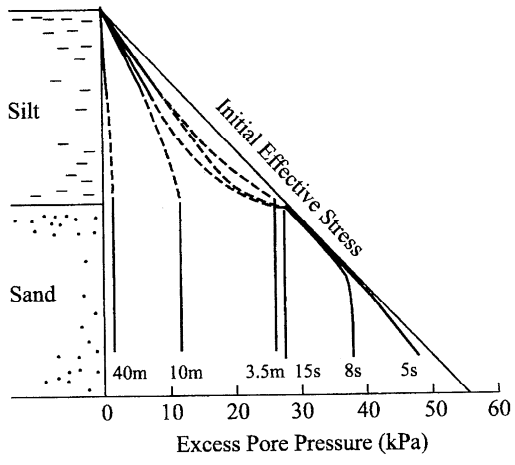

Fig. 5. Dissipation of excess porewater pressure during drainage (after Ref. [2]).

4.2. Simulation of centrifuge test

The simulation was conducted using the 1D program DESRA-2C [5] in which the joint element was incorporated. The modified program is designated DESRA-2CJ [6].

The simulation begins immediately after liquefaction has occurred in the sand. There are three distinct phases in the post-liquefaction behaviour of the centrifuge model as shown schematically in Fig. 6. In phase 1, the sand reconsolidates after liquefaction, leaving a film of water between the silt and the sand layers. In the short time required for this, little drainage takes place through the silt. In phase 2, the interlayer water film begins to drain through the silt and the silt layer begins to settle until finally it contacts the sand layer. During this phase, the porewater pressure in sand remains constant at the value in the joint. Phase 3 now begins in which the sand layer undergoes additional reconsolidation under the weight of the silt layer, until finally an equilibrium state is achieved.

The form of Eq. (20) and the expression of c in Eq. (21) are assumed to be valid for the test sand in the absence of any information on the post-liquefaction properties of that sand. The initial volumetric strain ϵ_{vo} for the reconsolidation analysis of the sand is calculated from the final settlement of the silt layer. This is considered a good approximation. The assumption is necessary because the LVDT to measure the sand settlement did not function properly during the test. The values of c and D in Eq. (20) are determined as explained earlier.

The reconsolidation analysis can now be conducted on the basis of Eqs. (19) and (23), beginning at the instant of liquefaction. All simulations are conducted at prototype scale. The permeabilities based on the laboratory tests

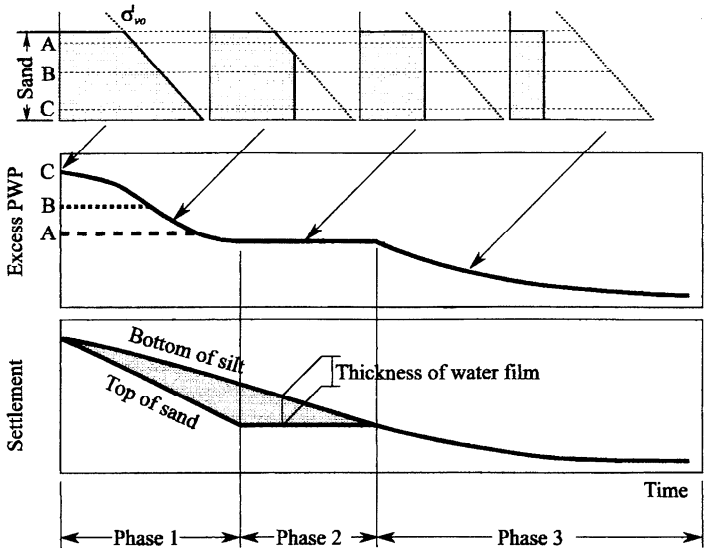

Fig. 6. Schematic representation of the three phases in the post-liquefaction behaviour of the layered system. A, B and C denote the locations where excess porewater pressure was measured. The relative durations of the various phases have been distorted to clearly show the short-duration early phases.

were used in the first trial simulation. The computed time-history of porewater pressure dissipation at the mid-height of the sand layer is shown in Fig. 7(a) for a duration of 50 s, in Fig. 7(b) for a duration of 10 min and in Fig. 7(c) for a duration of 60 min. The effective permeability of the sand in the centrifuge test after liquefaction must be greater than the $k = 1.065 \times 10^{-3}$ m/s measured on specimens of unliquefied sand because the computed time for maximum opening of the joint based on this permeability is about 25 s instead of the test value of about 15 s. A permeability of 2.13×10^{-3} m/s gives a good simulation of the test results as shown in Fig. 7(a). Such an increase in post-liquefaction permeability has also been noted by Arulanandan and Sybico [7].

The next phase is the drainage of the water layer through the silt. The test data indicate that the joint completely closes after about 4 min. For drainage through the silt a permeability of 8×10^{-5} m/s is necessary for the silt to make contact with the sand layer at the right time. This is 16 times greater than the measured permeability. The apparent increase in permeability may be due to cracks, which develop when the silt layer floats on the water or leakage of the contact between the silt and side of the centrifuge box.

For phase 3, in which the silt and sand are again in contact, the permeability of the silt must be reduced to 2×10^{-5} m/s for up to 10 min and then reduced to 5×10^{-6} m/s to get a good simulation. This reduction of permeability is consistent with the closing of cracks in the silt after contact with the sand.

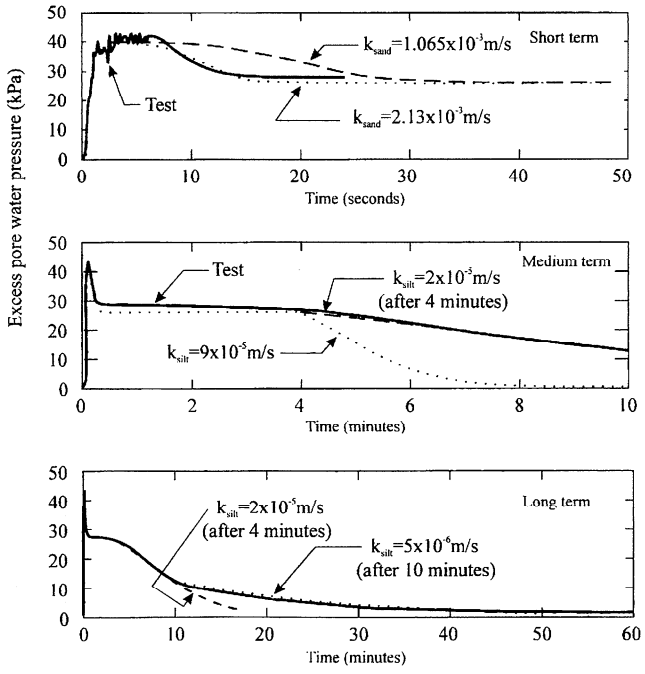

Fig. 7. Time-histories of porewater pressures over the short (0–50 s), medium (1–10 min), and long (0–60 min) terms.

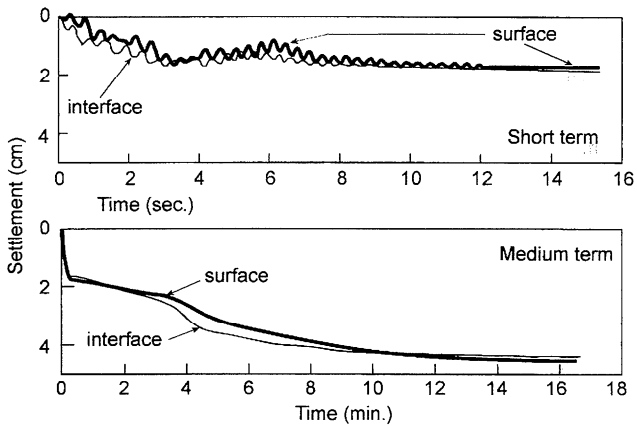

Fig. 8. Measured settlements in centrifuge test.

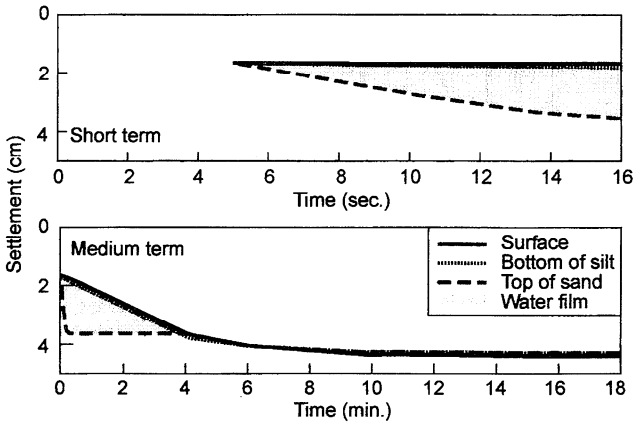

Fig. 9. Computer settlements in centrifuge test.

Fig. 8 shows measured settlements for both the short (0–16 s) and medium (0–18 min) terms. The settlements of the surface and the interface are nearly identical because the interface LVDT did not measure the sand settlement but remained attached to the bottom of the silt layer [2]. This means that there are no intermediate data available on the development on the thickness of the water film until the water film begins to dissipate through the silt. The abrupt occurrence of about 2 cm in the first 3–4 s is not compatible with the mechanics of the test model. It is most likely to be an initial adjustment in the upper layer and/or the LVDT. Fig. 9 shows the development of the water film and the contemporaneous settlement of the surface of the underlying sand layer in the short term, 0–16 s. The modelling starts at about 4 s, after the initial adjustments to the system noted above. In the medium term (also in Fig. 9) the water film begins to dissipate and the silt layer begins to approach the top of the sand layer. Contact is established at about 4 min, which seems to be a little later than that indicated by the interface curve in Fig. 8. Thereafter, as the porewater pressures dissipate, the effective stresses on the sand layer increase and additional settlements occur. Because of the problems of measuring the settlements accurately, reliable comparisons between measured and computed settlements as a function of time is not possible. However, comparisons between Figs. 8 and 9 suggest that the proposed method of analysis captures the evolving pattern of settlements rather well.

5. Conclusions

A joint element is presented for the analysis of what happens when a layer of sand liquefies beneath a relatively impermeable surface layer. The key responses that need to be modelled are the development and subsequent drainage of a film of water between the two layers, as the sand layer reconsolidates after liquefaction. The ability of the method to simulate the response of such a two-layer system in a Liu and Dobry centrifuge test [2] is encouraging.

The major impediment to a satisfactory validation of the method of analysis is a lack of data on the post-liquefaction properties of sand and some uncertainty about the actual performance of the model in the centrifuge test.

The joint element has been incorporated in the dynamic effective stress program DESRA-2CJ [6]. In theory, this allows the entire sequence of behaviour from the initiation of shaking to the final settlement to be followed. The model is being extended to 2D analysis.

Acknowledgements

The joint element project was supported by Sato Kogyo Company Ltd, Tokyo, Japan, and by a grant to the second author from the Natural Science and Engineering Research Council of Canada.

References

[1] Arulanandan K, Seed HB, Yogachandran C, Muralectharan KK, Seed RB, Kabiramany K. Centrifuge study on volume changes and dynamic stability of earth dams. ASCE Journal of Geotechnical Engineering 1993;119(11):1717–31.

[2] Liu L, Dobry R. Centrifuge earthquake modelling of liquefaction and its effect on shallow foundations. Department of Civil and Environmental Engineering, RPI, New York, 1993.

[3] Goodman RE, Taylor RL. A model for the mechanics of jointed rock. Journal of Soil Mechanics, ASCE 1968;94(SM3):637–59.

[4] Inadomaru K, Tsujino S, Yoshida N. Fundamental study on the residual settlement of ground after liquefaction [in Japanese]. In: Proceedings of the 49th Annual Conference of the Japan Society of Civil Engineering, vol III, 1994. p. 498–9.

[5] Finn, Liam WD, Lee MKW, Yoshida N. DESRA-2C, dynamic effective stress response analysis of layered deposits incorporating soil yielding. Department of Civil Engineering, University of British Columbia, Vancouver, BC, Canada, 1991.

[6] Finn, Liam WD, Yoshida N, Lee MKW. DESRA-2CJ, dynamic effective stress response analysis of layered deposits incorporating soil yielding. Department of Civil Engineering, University of British Columbia, Vancouver, BC, Canada, 1996.

[7] Arulanandan K, Sybico J. Post-liquefaction settlement of sand mechanism and in situ evaluation. In: Proceedings of the Fourth Japan–US Workshop on Earthquake Resistant Design of Lifeline Facilities and Countermeasures for Soil Liquefaction, Honolulu, Hawaii. Technical Report NCEER-92-0019, 1992. p. 239–47.